AIAA 99-4001
Force and Moment Approach for Achievable Dynamics using Nonlinear Dynamic Inversion

Aaron J. Ostroff and Barton J. Bacon
NASA Langley Research Center
Hampton, VA

AIAA Guidance, Navigation, and Control Conference

August 9-11,1999 /Portland, OR

FORCE AND MOMENT APPROACH FOR ACHIEVABLE DYNAMICS USING NONLINEAR DYNAMIC INVERSION

Aaron J. Ostroff and Barton J. Bacon
NASA Langley Research Center
Hampton, VA

Abstract

This paper describes a general form of nonlinear dynamic inversion control for use in a generic nonlinear simulation to evaluate candidate augmented aircraft dynamics. The implementation is specifically tailored to the task of quickly assessing an aircraft's control power requirements and defining the achievable dynamic set. The achievable set is evaluated while undergoing complex mission maneuvers, and perfect tracking will be accomplished when the desired dynamics are achievable. Variables are extracted directly from the simulation model each iteration, so robustness is not an issue. Included in this paper is a description of the implementation of the forces and moments from simulation variables, the calculation of control effectiveness coefficients, methods for implementing different types of aerodynamic and thrust vectoring controls, adjustments for control effector failures, and the allocation approach used. A few examples illustrate the perfect tracking results obtained.

Introduction

A key first step in any aircraft control law design is to determine a set of achievable dynamics that can be realized given the limitations of the vehicle's effectors to produce the required forces and moments. This is prudent since the results of such an analysis can guide the design and potentially avoid costly redesign further along the design process. In general, the set of aircraft dynamics known to promote good handling is expressed in terms of linear transfer functions. Ideally, the good handling set should intersect the achievable set and the designer should strive to augment the vehicle dynamics to be within this intersection. The danger of augmenting the vehicle dynamics to be outside this intersection is rate-limited actuators and potential PIO tendencies [1,2]. Sometimes there is no intersection: limitations of the vehicle prevent augmenting it to have good handling qualities. In that case, control power requirements (e.g. surface sizing, control allocation) need to be reexamined before proceeding to a detailed control law design. Clearly, regardless of the result, this sort of analysis is better done sooner than later. The objective of this paper is to describe development of a tool capable of determining the set of achievable dynamics as early in the design process as possible.

The approach proposed utilizes a general form of nonlinear dynamic inversion (NDI) control in a generic nonlinear simulation tool to realize and test candidate augmented aircraft dynamics. Here, the implementation is specifically tailored to the task of quickly assessing an aircraft's control power requirements and defining the achievable set. Smith [3,4] previously proposed this application of NDI. The work presented here is an extension of that work to address various response types and incorporate handling quality specifications. Similar to Smith's approach, the equations of motion are directly manipulated to provide controls yielding desired responses for select control variables. Here, the control variables are not limited to angular body rates but can directly include contributions from angle of attack and sideslip angle to modify control power requirements. As done in other works [3,5], the ultimate objective here is a rapid prototyping tool capable of establishing control design guidelines without the costly investment of a detailed conventional control design. A high performance airplane model with multiple innovative control effectors is used to demonstrate this tool.

Several noteworthy features and uses of the proposed Force/Moment NDI approach are listed below.

1. This nonlinear simulation analysis tool gives the best possible tracking for a desired set of dynamics, and can be used to determine the set of achievable dynamics while maneuvering over the entire flight envelop either in batch or real-time piloted simulation.
2. The control law does not require adjustment, with the exception of selecting weights if a control allocation approach is used.
3. Robustness is not an issue since variables, in particular force and moment increments, are extracted directly from the simulation model and functional fits are not required.
4. Candidate low-order augmented aircraft responses, as defined in the Mil Standard [6], can easily be used and varied for evaluation.

5. Other uses include evaluation of control allocation techniques, development of guidelines for reconfigurable control, and evaluation of new control effector concepts that are presently being explored [7,8].
6. The tool's format allows quick and easy comparison of various aerodynamic databases.

For this development, actuator dynamics are not included, but rate and position limits are considered.

The main point of each section, corresponding to the order presented in this paper is 1)an overview of nonlinear dynamic inversion control as it pertains to this particular application, 2)manipulation of the aircraft's equations of motion to provide the required inner-loop control, 3)extraction of the required force and moment data, 4)discussion of the inverse control map for generating pseudo surface commands, 5)the pseudo inverse allocation approach used, 6)implementation of the aerodynamic coefficients to account for control effector failures, 7)calculation of the control power required, 8)non-minimum phase analysis, and 9)presentation of illustrative examples.

Nonlinear Dynamic Inversion Control

In this section, an overview of the control is offered followed by a more detailed description of the control's respective parts. The general form of the control law, shown in figure 1, is not too different from previously applied NDI control approaches [9,10]. Due to the information available from the simulation, however, the implementation here will be greatly simplified over reference 9.

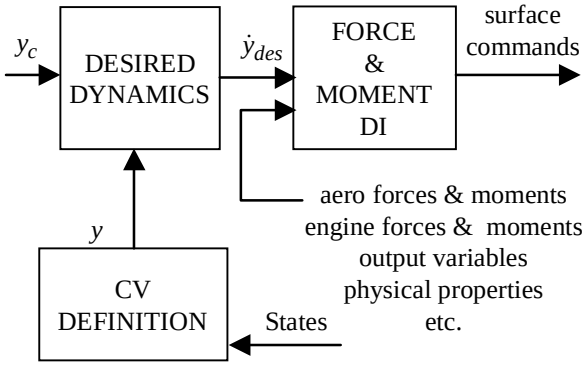

Figure 1. Overview of Control Law.

The control consists of two parts: 1) control variable (CV) processing and 2) dynamic inversion (DI). Control variable processing consists of the CV definition and the CV rate command generation. The overall control objective is to achieve some desired response of the CV vector y to command y_c. Various states are typically blended to define the elements of y. Generally, there are three elements corresponding to motion about each of the three axes: longitudinal, lateral, and directional. The command y_c, of the same dimension as y, can be thought of as the result of shaping and filtering (not shown) of the pilot's stick and pedal inputs. These control variables and their commands are fed to a block that processes the signals to produce the desired responses (actually rates of the desired responses). The desired response signals are, in turn, fed to the DI block that issues the required surface commands to produce the desired responses from the actual vehicle. Essentially, the DI block makes the transfer function matrix from $\dot{y}_{des}$ to y an integrator, i.e., diagonal matrix with first-order integrators. As a result, the actual control variables equal the desired ones subject to the vehicle's control power constraints.

This partitioning of control makes the strategy for determining the achievable set straightforward. The control variable processing portion of the control law, CV definition and desired dynamics, produces desired responses for the candidate low-order command models that are decoupled along axes and compliant with the military specification. The dynamic inversion portion of the control law generates surface commands to produce the desired response from the vehicle subject to its control power limitations. Note the set of achievable dynamics consists of the low-order command models that the vehicle is capable of following.

Control Variable Processing

Assume there are three control variables corresponding to some desired motion about the longitudinal, lateral, and directional axes

$$y = [y_{lon}, y_{lat}, y_{dir}]^T . \quad (1)$$

Let x denote the state of the aircraft in the generic simulation whose motion is governed by

$$\dot{x} = F(x, \delta) . \quad (2)$$

For this paper, assume that $\dim(\delta) \geq \dim(y)$ and the control variable is related to the state as

$$y = h(x) . \quad (3)$$

Here, $x = [u \quad w \quad q_b \quad \theta \quad v \quad p_b \quad r_b \quad \phi]^T$ where (u, v, w) and (p_b, q_b, r_b) are respectively the components of the aircraft's translational and angular velocity expressed in body axes. The standard Euler angles (θ, ϕ) are used to orient the gravitational force to the body axes. The control δ will be described later.

To facilitate the upcoming discussion, an auxiliary set of states x_{aux} that is linearly related to the control variables is introduced as

$$y = Hx_{aux} \quad (4)$$

where H is a constant matrix. Assume $x_{aux} = f_{aux}(x)$ so that $h(x) = Hf_{aux}(x)$. The auxiliary set can include such variables as angle of attack, sideslip angle and stability axis components of angular velocity in addition to any of the original states.

In figure 1, the control variables and y_c are fed into a block labeled 'desired dynamics'. This block defines the desired dynamic behavior the control variables should follow. Assuming the inner DI loop has produced a decoupled integrator block relating $\dot{y}_{des}$ to y, the three loops may be considered separately in defining the 'desired dynamics' block. Here, three command models define the augmented vehicle dynamics in the longitudinal, lateral, and directional axes respectively as:

$$\frac{y_{lon,des}}{\delta_{lon}} = \frac{K_{lon}\omega_{lon}^2(s+\omega_{n,lon})}{s^2+2\zeta_{lon}\omega_{lon}s+\omega_{lon}^2} \tag{5}$$

$$\frac{y_{lat,des}}{\delta_{lat}} = \frac{\omega_{lat}}{s+\omega_{lat}} \tag{6}$$

$$\frac{y_{dir,des}}{\delta_{dir}} = \frac{\omega_{dir}^2}{s^2+2\zeta_{dir}\omega_{dir}s+\omega_{dir}^2}. \tag{7}$$

Transfer functions selected for these command models are typical transfer functions found in the military specifications. [6] These low-order responses can be achieved using an outer-loop control structure as illustrated for the longitudinal axes in figure 2. The integrator resulting from dynamic inversion of the simulated vehicle is shown in the figure with an approximation sign.

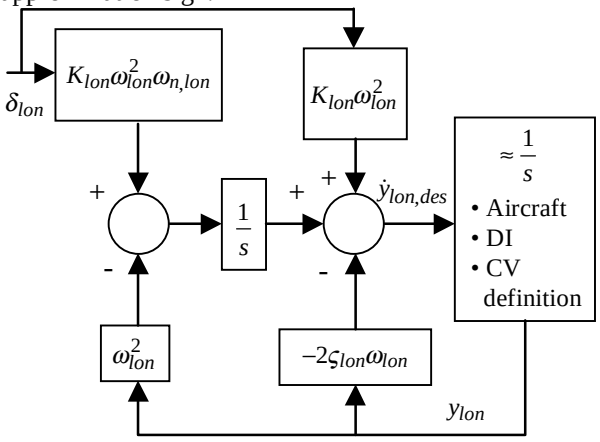

Figure 2. Details of Longitudinal Outer-loop Control.

It should be mentioned that as long as the control effectors remain within their respective rate and position limits and they generate forces and moments that are linear with respect to their deflections, dynamic inversion will produce the required integrator. Moreover, the desired dynamics will be realized. This statement assumes the control variables chosen promote internal stability which will be addressed in a later section. Here, robustness to model uncertainty is not an issue since the dynamics are known exactly in the simulation. Robustness could be an issue, however, when the control is no longer linearly related to its generated moments and forces. In that case, the inverse control mapping to be proposed will lead to an approximate integrator.

Dynamic Inversion

The purpose of the DI block in figure 1 is to generate the proper control inputs such that the set of desired dynamics is achieved. Generally, the simulation's force and moment build up in the equations of motion are such that increments due to controls can be separated from those due to the baseline aircraft moving through the air mass. Specifically, equation (2) can be expressed as

$$\dot{x} = f(x) + g_1(x,\delta). \tag{8}$$

Dynamic inversion, however, assumes that the control's influence is linear or

$$\dot{x} = f(x) + g(x)\delta. \tag{9}$$

To realize the control that achieves a desired control variable response y_{des} for this system, take the derivative of y using equation (3) as

$$\dot{y} = \frac{\partial h(x)}{\partial x}\dot{x} = h_x f(x) + h_x g(x)\delta \tag{10}$$

where $h_x = \partial h(x)/\partial x$. When the number of control variables and control effectors are equal, the dynamic inversion control may be solved for directly as

$$\delta_{cmd} = (h_x g(x))^{-1}(\dot{y}_{des} - h_x f(x)). \tag{11}$$

In the usual case where the number of effectors is greater then the number of control variables, some type of control allocation method is required. A weighted pseudo inversion approach is discussed later in this paper.

Dynamic inversion assumes that the inverse control mapping $(h_x g(x))^{-1}$ exists. If $h_x g(x)$ is nearly singular, the set of effectors are either redundant or ill suited to force the selected control variables to follow a desired response. Dynamic inversion also assumes that the control variables chosen will not produce unstable internal dynamics (discussed later in paper). Dynamic inversion only guarantees the response of y to y_c, but this assumes the dynamics unobserved in y remain stable. It is clear that if these assumptions are satisfied then the dynamic inversion control produces $\dot{y}_{des} = \dot{y}$.

Figure 3 shows the dynamic inversion portion of the control for the system of equation (9). The function $f(x)$ contains the accelerations due to the forces and moments generated by the baseline vehicle as it moves through the air mass. It should be mentioned that the

function $f(x)$ also contains the inertial and gravitational components of acceleration. If one were to implement the NDI control [9], functional approximations of the aerodynamic database would have to be carried in the control along with a reconstruction of the inertial and gravitational components of acceleration. In this application, however, the aerodynamic forces and moments are reconstructed from their respective non-dimensional coefficients taken directly from the simulation. That is why in figure 1 forces and moments are being fed directly to the 'DI' block. An actual implementation of NDI control would have to operate only on sensor measurements.

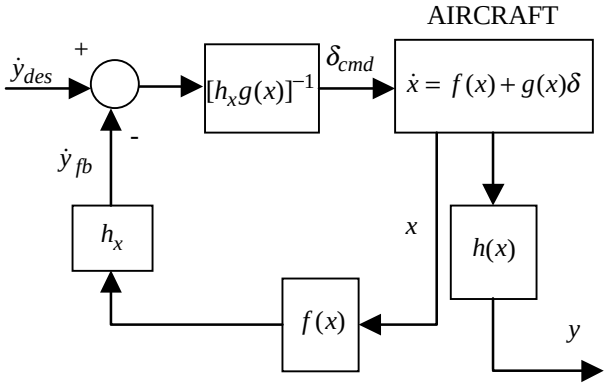

Figure 3. NDI Inner-Loop (Linear Controls)

Let us consider the inverse nonlinear control corresponding to the actual equation of motion found in equation (8). The inverse control must satisfy

$$\dot{y}_{des} - h_x f(x) = h_x g_1(x, \delta_{cmd}) \tag{12}$$

to make $\dot{y}_{des} = \dot{y}$. An approximation, discussed in a later section, is used in this paper. Prior to considering this feed-forward portion of the control, the simulation's equations of motion are manipulated to provide the required feedback signal.

Force and Moment Approach to Dynamic Inversion

This section includes key equations for the force and moment approach to nonlinear dynamic inversion (NDI). A standard x-y-z body axes coordinate frame is used. Presented below are the nonlinear force and moment equations [11] for a flat-earth, rigid-body, symmetrical airplane.

$$\begin{aligned}
&X - mg\sin\theta = m(\dot{u} - vr_b + wq_b)\\
&Y + mg\sin\phi\cos\theta = m(\dot{v} + ur_b - wp_b)\\
&Z + mg\cos\phi\cos\theta = m(\dot{w} - uq_b + vp_b)\\
&L = I_{xx}\dot{p}_b - I_{xz}\dot{r}_b - I_{xz}p_b q_b + (I_{zz} - I_{yy})r_b q_b\\
&M = I_{yy}\dot{q}_b + (I_{xx} - I_{zz})p_b r_b + I_{xz}(p_b^2 - r_b^2)\\
&N = I_{zz}\dot{r}_b - I_{xz}\dot{p}_b + (I_{yy} - I_{xx})p_b q_b + I_{xz}q_b r_b
\end{aligned} \tag{13}$$

Here X, Y, and Z represent the total aerodynamic and thrust forces (lb), L, M, and N represent the total aerodynamic and thrust moments (ft-lb); I_{xx}, I_{yy}, I_{zz}, and I_{xz} are the moments and product of inertia (slug-ft^2); m is the mass (slugs); u, v, and w represent the linear velocities (ft/s); $\dot{u}$, $\dot{v}$, and $\dot{w}$ are the respective linear accelerations (ft/s^2); p_b, q_b, and r_b represent the roll, pitch, and yaw rates (rad/s); and $\dot{p}_b$, $\dot{q}_b$, and $\dot{r}_b$ are the respective angular accelerations (rad/s^2).

As stated previously, the control forces and moments must be separated from all other aerodynamic and thrust forces and moments. Using this separation and solving for the modified acceleration terms yield

$$\begin{aligned}
\dot{u}_{ae} &= \frac{X - X_\delta}{m} - g\sin\theta + vr_b - wq_b\\
\dot{v}_{ae} &= \frac{Y - Y_\delta}{m} + g\sin\phi\cos\theta - ur_b + wp_b\\
\dot{w}_{ae} &= \frac{Z - Z_\delta}{m} + g\cos\phi\cos\theta + uq_b - vp_b\\
\dot{q}_{b,ae} &= \frac{1}{I_{yy}}\begin{Bmatrix}(M - M_\delta) - (I_{xx} - I_{zz})p_b r_b\\ -I_{xz}(p_b^2 - r_b^2)\end{Bmatrix}\frac{180}{\pi}\\
\begin{Bmatrix}\dot{p}_{b,ae}\\ \dot{r}_{b.ae}\end{Bmatrix} &= \begin{bmatrix} I_{xx} & -I_{xz}\\ -I_{xz} & I_{zz}\end{bmatrix}^{-1}\\
&\quad\begin{Bmatrix} L - L_\delta + I_{xz}p_b q_b - (I_{zz} - I_{yy})r_b q_b\\ N - N_\delta - (I_{yy} - I_{xx})p_b q_b - I_{xz}q_b r_b\end{Bmatrix}\frac{180}{\pi}
\end{aligned} \tag{14}$$

where the subscript ae refers to aerodynamic, engine, inertial and gravitational accelerations only (no control accelerations) and the subscript δ represents control terms. In equations (14), the angular accelerations are converted to units of deg/s^2. All of the aerodynamic components are extracted from the simulation. This approach, as well as modeling of the thrust control terms, will be described in a following section.

Define the state vector x_{ae} as

$$x_{ae} = [u_{ae}, w_{ae}, q_{b,ae}, \theta, v_{ae}, p_{b,ae}, r_{b,ae}, \phi]^T. \tag{15}$$

In order to construct $f(x)$ the Euler auxiliary equations

$$\dot{\theta} = q_b\cos\phi - r_b\sin\phi \tag{16a}$$

$$\dot{\phi} = p_b + q_b\tan\theta\sin\phi + r_b\tan\theta\cos\phi \tag{16b}$$

which contain no explicit reference to control forces and moments, are added to the set in equations (14) yielding

$$\dot{x}_{ae} = f(x). \tag{17}$$

The same $f(x)$ is defined in equations (8) and (9). Assuming the control variable is defined as in equations (3) and (4), the NDI feedback of figure 3 can be expressed as

$$\dot{y}_{fb} = h_x f(x) = h_x\dot{x}_{ae} = H\frac{\partial x_{aux}}{\partial x}\dot{x}_{ae} \tag{18}$$

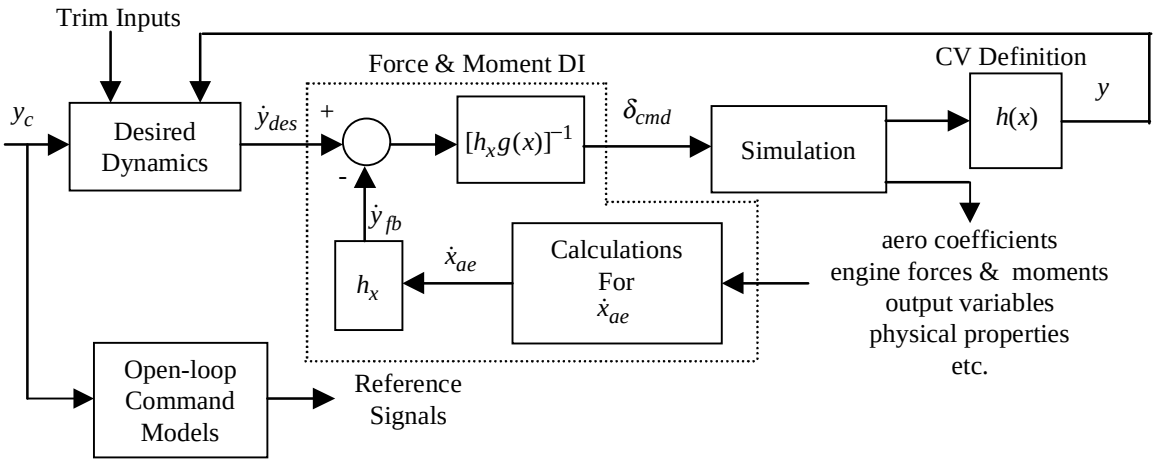

Figure 4. Combined NDI configuration.

A typical set of auxiliary states that could be used to form the control variables is

$$x_{aux} = [\alpha, q_b, \beta, p_s, r_s]^T \tag{19}$$

where α and β represent the angles of attack and sideslip respectively, and p_s and r_s represent stability axis roll and yaw rates respectively. Obviously, these x_{aux} variables do not form a complete set of possible controlled outputs, but are used here as an example.

In vectors x_{ae} and x_{aux}, velocities have units of ft/s and angular variables have units of degrees. The partial differential $\partial x_{aux} / \partial x$ is defined below in matrix form for the elements shown in equations (15) and (19) as

$$\frac{\partial x_{aux}}{\partial x} = \begin{bmatrix} \frac{\partial \alpha}{\partial u} & \frac{\partial \alpha}{\partial w} & 0 & 0 & 0 & 0 & 0 & 0 \\ 0 & 0 & 1 & 0 & 0 & 0 & 0 & 0 \\ \frac{\partial \beta}{\partial u} & \frac{\partial \beta}{\partial w} & 0 & 0 & \frac{\partial \beta}{\partial v} & 0 & 0 & 0 \\ \frac{\partial p_s}{\partial u} & \frac{\partial p_s}{\partial w} & 0 & 0 & 0 & \frac{\partial p_s}{\partial p_b} & \frac{\partial p_s}{\partial r_b} & 0 \\ \frac{\partial r_s}{\partial u} & \frac{\partial r_s}{\partial w} & 0 & 0 & 0 & \frac{\partial r_s}{\partial p_b} & \frac{\partial r_s}{\partial r_b} & 0 \end{bmatrix} \tag{20}$$

and the solution to the first derivative is illustrated as

$$\frac{\partial \alpha}{\partial u} = \frac{-w}{u^2 + w^2} \frac{180}{\pi} \tag{21}$$

where the units are deg/ft/sec. Equation (20) is used to solve equation (18) for h_x. Figure 4 illustrates how the variables described fit into the NDI closed-loop structure.

Extraction of Force and Moment Data from Simulation

Aerodynamic Variables

In the typical airplane simulation, force and moment aerodynamic data are defined in tables that are generated from wind tunnel and flight data. These tables, which require interpolation, usually contain non-dimensional coefficients (c_i) that are nonlinear functions of many airplane variables, for example α, β, Mach, altitude, and δ. The aerodynamic forces and moments that affect aircraft stability (no control contributions) are then calculated as

$$\begin{aligned} X_a &= (c_x - c_{\delta x})\bar{q}S \\ Y_a &= (c_y - c_{\delta y})\bar{q}S \\ Z_a &= (c_z - c_{\delta z})\bar{q}S \\ L_a &= (c_l - c_{\delta l})\bar{q}Sb \\ M_a &= (c_m - c_{\delta m})\bar{q}S\bar{c} \\ N_a &= (c_n - c_{\delta n})\bar{q}Sb \end{aligned} \tag{22}$$

where $\bar{q}$ is dynamic pressure (lb/ft^2), S is the wing reference area (ft^2), b is the wing span (ft), and $\bar{c}$ is the mean aerodynamic chord (ft). Aerodynamic forces X_a, Y_a, Z_a have units of lb and the aerodynamic moments L_a, M_a, N_a have units of ft-lb. The coefficients (c_x, c_y, c_z) represent the total non-dimensional aerodynamic force along each axis and coefficients (c_l, c_m, c_n) represent the total non-dimensional aerodynamic moment about the corresponding axis. The c_δ terms are the non-dimensional aerodynamic force and moment coefficients due to controls. Note that the total non-dimensional coefficients include the c_δ terms, so these control contributions are just being subtracted out. In this paper, the c_δ terms also include interference coefficients for the appropriate control effectors. In a later section, it will be shown how the c_δ coefficients are used to create the feed-forward portion of the control.

Thrust Variables

Thrust vectoring is applied to both the pitch and yaw axes. Here, the control components $(X_{\delta t}, Y_{\delta t}, Z_{\delta t}, L_{\delta t}, M_{\delta t}, N_{\delta t})$ resulting from the yaw nozzle deflection δ_{ty} and pitch nozzle deflection δ_{tp} are calculated as

$$\begin{aligned} X_{\delta t} &= T_g\left(\cos(\delta_{tp})\cos(\delta_{ty})-1\right) \\ Y_{\delta t} &= T_g\cos(\delta_{tp})\sin(\delta_{ty}) \\ Z_{\delta t} &= -T_g\sin(\delta_{tp}) \\ L_{\delta t} &= -l_z Y_{\delta t} \\ M_{\delta t} &= l_x Z_{\delta t} + l_z X_{\delta t} \\ N_{\delta t} &= -l_x Y_{\delta t} \end{aligned} \tag{23}$$

where l_x is the distance (ft) of the nozzle force behind the cg, l_z is the distance (ft) below the waterline, and T_g represents gross thrust (lb). These functional equations will be used to develop an approximate inverse controls map.

Combined Forces and Moments

The combined aerodynamic and engine forces and moments in equations (14) are calculated by using results from equations (22) and (23) as

$$\begin{aligned} X - X_\delta &= X_a + X_t - X_{\delta t} \\ Y - Y_\delta &= Y_a + Y_t - Y_{\delta t} \\ Z - Z_\delta &= Z_a + Z_t - Z_{\delta t} \\ L - L_\delta &= L_a + L_t - L_{\delta t} \\ M - M_\delta &= M_a + M_t - M_{\delta t} \\ N - N_\delta &= N_a + N_t - N_{\delta t} \end{aligned} \tag{24}$$

where $(X_t, Y_t, Z_t, L_t, M_t, N_t)$ represent the total thrust forces and moments, and the other variables have been previously defined.

Inverse Control Map

Previous sections involved constructing suitable expressions for $\dot{y}_{des}$ and $h_x f(x)$. In this section, equation (12) is solved using an approximation of g_1 that is linear with respect to the present control, or $g_1 \cong g_B\delta$. Standard linear inverse operations (standard inverse or minimum norm solution), where g_B replaces $g(x)$ of figure 3, define the feed-forward path of the proposed NDI control.

From the equations of motion, the accelerations due to all controls define $g_1(x,\delta)$, or

$$\begin{aligned} \dot{u}_\delta &= X_\delta/m \\ \dot{w}_\delta &= Z_\delta/m \\ \dot{q}_\delta &= (M_\delta/I_{yy})(180/\pi) \\ \dot{v}_\delta &= Y_\delta/m \\ \dot{p}_\delta &= (I_{zz}L_\delta + I_{xz}N_\delta)(180/\pi)/\bar{I} \\ \dot{r}_\delta &= (I_{xz}L_\delta + I_{xx}N_\delta)(180/\pi)/\bar{I} \end{aligned} \tag{25}$$

where $\bar{I} = I_{xx}I_{zz} - I_{xz}^2$. The aerodynamic controls δ_a and thrust vectoring controls δ_{tv} independently generate forces and moments, so for example

$$X_\delta = X_{\delta a} + X_{\delta t} \tag{26}$$

where $X_{\delta a}$ denotes the force in x-direction due to total aerodynamic control. As a result, $g_1(x,\delta)$ expands as

$$g_1(x,\delta) = g_a(x,\delta_a) + g_{tv}(x,\delta_{tv}). \tag{27}$$

Further expansion, however, is limited due to controls in δ_a and δ_{tv} whose effectiveness is determined by the position of other controls. This control dependency is dealt with in the next two subsections as linear control approximations are sought separately for g_a and g_{tv}.

Aerodynamic Controls Map Approximation

From equations (25) and (26) and the form of (22), linear control approximations are actually sought for the total control force and moment coefficients to generate a $g_{a,B}$ so $g_a \cong g_{a,B}\delta_a$. Let $c_{\delta m}$ serves as an example.

In the aerodynamic database, the total pitch moment control coefficient expands as

$$\begin{aligned} c_{\delta m}(x,\delta_a) = &\sum_{i=1}^{l_1} c_{\delta m,i}(x,\delta_i) + \sum_{i=l_1+1,\, i\neq j}^{l_a} c_{\delta m,i}(x,\delta_i,\delta_j) \\ &+ \sum_{i\neq j} c_{\delta m,\mathrm{int},ij}(x,\delta_i,\delta_j) \end{aligned} \tag{28}$$

where $\delta_a = (\delta_1, \cdots, \delta_{la})^T$. The first two sets of coefficients on the right side of the equation vanish only when the primary control δ_i is zero. The third set, the interference coefficients, vanish whenever $\delta_i = 0$ or $\delta_j = 0$. Similar expressions with the same number of coefficients and their respective dependent variable sets exist for the other total control force and moment coefficients.

Let δ_i^0 denote the previous value of δ_i and assume, for the moment, that an intermediate call has been made to the aerodynamic database to retrieve coefficients evaluated at the current state x and the previous control, e.g. $c_{\delta m,i}(x,\delta_i^0,\delta_j^0)$. For the non-interference coefficients, a simple linear control approximation $\tilde{c}_{\delta m,i}$ results from dividing the intermediate coefficient by its previous primary control, i.e.,

$$\tilde{c}_{\delta m,i}(x,\delta_i) = (c_{\delta m,i}(x,\delta_i^0)/\delta_i^0)\delta_i \tag{29}$$

$$\tilde{c}_{\delta m,i}(x,\delta_i,\delta_j) = (c_{\delta m,i}(x,\delta_i^0,\delta_j^0)/\delta_i^0)\delta_i. \tag{30}$$

This 'global slope' approximation is viable here because: 1)the integration time step Δt is generally small, and 2)each effector is rate limited, $|\dot{\delta}_i| \le \dot{\delta}_{i,\max}$. The combination implies that the neighborhood about $(\delta_i^0, \delta_j^0, \ldots)$ where (29) and (30) must hold is small being limited by the effector's maximum travel, i.e. $\Delta_{i,\max} = \Delta t \cdot \dot{\delta}_{i,\max}$, from its previous value.

Figure 5 illustrates the approximation for $c_{\delta m,i}(x, \delta_i, \delta_j)$ over the neighborhood of possible travel of δ_i and δ_j. The shaded area corresponds to $c_{\delta m,i}$ evaluated at all points in the neighborhood. The dashed line is the approximation expressed in equation (30). Here, linear interpolation is assumed and the neighborhood does not cross any tabular breakpoints of δ_i and δ_j. Under these assumptions, the slope of $c_{\delta m,i}$ is constant along paths of constant δ_i and constant δ_j. For any δ_i where $|\delta_i - \delta_i^0| \le \Delta_{i,\max}$, it can be shown that the approximation error is bounded as

$$|c_{\delta m,i} - \tilde{c}_{\delta m,i}| \le |S_{iG} - S_i| \cdot \Delta_{i,\max} + |S_j| \cdot \Delta_{j,\max} \qquad (31)$$

where $S_{iG} = c_{\delta m,i}/\delta_i$, $S_i = \partial c_{\delta m,i}/\partial \delta_i$ for $\delta_i = \delta_i^0$ and $\delta_j = \delta_j^0$, and $\overline{S}_j$ is the steepest $\partial c_{\delta m,i}/\partial \delta_j$ for $\delta_j = \delta_j^0$ at the extreme travel of δ_i, i.e. $\delta_i^0 \pm \Delta_{i,\max}$. Note the first term on the right of (31) corresponds to the difference between the global slope and the local slope along δ_i. Both terms on the right are weighted by the maximum excursion of the respective control.

Expression (31) can also be applied to the other coefficients in (28). For $c_{\delta m,i}(x, \delta_i)$, the second term vanishes. For the interference terms $c_{\delta m,\text{int},ij}$, the coefficient vanishes when either control equals zero. Either control could be assumed to be primary, so

$$\tilde{c}_{\delta m,\text{int},ij} = (c^0_{\delta m,\text{int},ij} / \delta_i^0)\delta_i \text{ or } (c^0_{\delta m,\text{int},ij} / \delta_j^0)\delta_j \qquad (32)$$

where $c^0_{\delta m,\text{int},ij} = c_{\delta m,\text{int},ij}(x, \delta_i^0, \delta_j^0)$. Ideally, it would be the one leading to the smallest error bound in (31). The linear control approximation of $c_{\delta m,i}$ is then obtained by substituting the coefficients of equations (29), (30), and (32) into equation (28). Analogous expressions can be developed to approximate the other total force and moment coefficients. Dimensionalized and substituted into equations (25) and (26), these approximate coefficients yield the desired input map

$$g_a(x, \delta_a) \cong g_{a,B}(x, \delta_a^0)\delta_a . \qquad (33)$$

Here, it is assumed that the previous primary controls are nonzero. When one is zero, the effectiveness due to the last nonzero control is used.

To speed up implementation, the previous state x^0 was substituted above for the current state on right side of equation (33). Due to the slow-varying nature of the state-related dependent variables (e.g. Mach, α, β) relative to the time step $\Delta t = .01\text{sec}$, no noticeable differences were observed in practice. Moreover, in the feedback path, the aerodynamic force and moment coefficients representing the baseline with no controls also used previous values with no problems. This simplification essentially delayed the non-inertial portion of the feedback signal by 10 msec. Using the previous coefficients in constructing the feedback path and the approximate linear control map for the feed-forward portion, a very efficient procedure was realized in implementing this NDI tool. The efficiency realized, moreover, could not be obtained using functional fits, incremental implementations requiring tables of partial derivatives, or additional calls to the aerodynamic data base to get the present force and moment information.

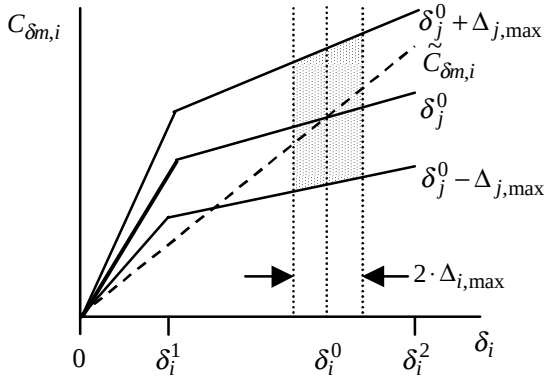

Figure 5. Linear control approximation of $c_{\delta m,i}$.

Thrust Vectoring Controls Map Approximation

As before, linear control approximations are sought for the thrust vectoring control forces and moments. Unlike the aerodynamic control coefficients, the control force and moments due to thrust vectoring have functional descriptions (eq. (23)).

The procedure used here involves local slopes based on the previous control. The linear control approximation of $X_{\delta t}$, for example, has the form

$$\tilde{X}_{\delta t} = \frac{\partial X_{\delta t}}{\partial \delta_{ty}}\Big|_{\delta_{ty}^0, \delta_{tp}^0} \delta_{ty} + \frac{\partial X_{\delta t}}{\partial \delta_{tp}}\Big|_{\delta_{ty}^0, \delta_{tp}^0} \delta_{tp} . \qquad (34)$$

To be noted, this form is not motivated by a Taylor series expansion of $X_{\delta t}$ about zero thrust vectoring controls. For a limited deflection range ($\le 15°$), analysis showed it to be as good as the Taylor series expansion. Moreover, in practice it proved better than a 'global slope' approach patterned after that used in the previous section.

Analogous expressions to (34) for the other thrust vectoring forces and moments, substituted into equations (25) and (26), yield the desired linear control

approximation form for $g_{tv}(x,\delta_{tv})$. Combined with results of the last section, the linear control approximation of $g_1(x,\delta)$ then is

$$g_1(x,\delta) \cong g_{B,a}\delta_a + g_{B,tv}\delta_{tv} = g_B\delta \tag{35}$$

where matrices $g_{B,a}$, $g_{B,tv}$, and g_B are evaluated at the previous state and control. Above, the control map assumes that each control can have positive and negative deflections. Prior to establishing the inverse control map, controls restricted to unilateral deflections (positive or negative) are briefly considered.

Unilateral Control Map Approximation

In this paper, it is assumed there is always a left-right pair of unilateral controls. Here, the nominal method used to operate this type of control is to either use the left control or the right control, but not at the same time. This is accomplished by designating a pseudo control in which a negative command moves, for example, the right control and a positive command moves the left control. As an illustration, let $\delta_{3R,L}$ designate a unilateral right/left control pair and δ_3 the pseudo control. Since only the right or left control will be nonzero, the pair's contribution to the total pitch moment control can be approximated as

$$c_{\delta m,3R} + c_{\delta m,3L} \cong \frac{\left(c_{\delta m,3L}(x^0,\delta_{3L}^0) + c_{\delta m,3R}(x^0,\delta_{3R}^0)\right)}{\delta_{3L}^0 - \delta_{3R}^0}\delta_3 \tag{36}$$

Here a negative value of δ_3 corresponds to the deflection of the right control and a positive value of δ_3 corresponds to the left control. In the approximation of equation (35), equation (36) implies that the columns of $g_{B,a}$, corresponding to δ_{3L} and δ_{3R}, are replaced with one corresponding to δ_3.

Pseudo Inverse Allocation

The typical airplane control system has more control effectors than control variables, so some type of allocation approach is required to distribute the control commands. In this paper, a weighted pseudo inverse approach is used. With fewer equations than unknowns in equation (12) given (35), minimize $\delta^T W^{-1}\delta$ in the solution to yield the inverse control map

$$\delta = W(h_x g_B)^T \left[h_x g_B W(h_x g_B)^T\right]^{-1} z \tag{37}$$

where $z = \dot{y}_{des} - h_x f(x)$. The weighting matrix, W, along with the control variables are the only variables that the designer must adjust in the entire control process. Here, for example, the diagonal elements of W consist of the rate limits $\dot{\delta}_{i,\max}$. As a result, the controls with the higher rate limits will be utilized more in the dynamic inversion control.

For unilateral controls, the resulting psuedo control must be correctly translated into left and right control commands. The left side is chosen when the pseudo control command is positive and the right side is chosen when the pseudo control command is negative.

Adjustment for Control Effector Failures

The tool has potential application in determining achievable dynamics in the face of control effector failures. This requires changes both to the feedback and feed-forward portions of the dynamic inversion control.

Control effector failures can occur in several forms such as stuck position, missing or partially missing surfaces, and floating surfaces. When a control failure occurs, forces and moments generated by that control must be included with the corresponding NDI feedback signals when the effector is no longer used for control. For example, suppose the i^{th} primary control (first term in eq. (28)) fails and that this control also has interference aerodynamics (third term in eq. (28)). All force and moment non-dimensional aerodynamic coefficients shown in eq. (22) will be modified, but for simplicity only the pitching moment equation will be illustrated as

$$M_a = (c_m - c_{\delta m} + c_{\delta m,i} + c_{\delta m,\text{int},ij})\bar{q}S\bar{c} \tag{38}$$

showing how the failed control moment increments are taken into account.

The following changes are required in the feed-forward NDI path. When a bilateral control fails, W_i is set to zero, thus eliminating the i^{th} control command. Options for a unilateral control are to either eliminate the opposite side (left or right side) after a failure by setting $W_i = 0$, or to use the opposite side to counteract forces and moments generated by the failed control if that control has a non-zero deflection. The latter option has been selected for a stuck actuator and the former option for a missing surface.

Power Required

One feature of this achievable-dynamics approach is the ability to measure the control power required when flying complex trajectories. The method used in this paper is to multiply the g_B control effectiveness matrix by the reconstructed control command vector. The reason to reconstruct the control command vector is because actuator rate and position limits are used at the output of the pseudo inverse allocation. When these limits are reached, the control commands are modified accordingly. Mass and inertia terms are taken into account to calculate forces in units of pounds and moments in units of foot-pounds.

Non-Minimum Phase Analysis

Stability of the force and moment DI control is considered at various trim conditions in the flight envelope. To perform this analysis, recall dynamic inversion was basically implemented using an approximation of the nonlinear system, or

$$\begin{aligned} \dot{x} &= f(x) + g_B(x, \delta^0)\delta \qquad x \in R^n, \delta \in R^l \\ y &= h(x) \qquad\qquad\qquad y \in R^m \end{aligned} \tag{39}$$

where δ^0 refers to the previous control. Here, the previous state in the control map has been replaced with the current one. Let the previous state/control $\{x^0, \delta^0\}$ represent a trim condition of (39), i.e.

$$0 = f(x^0) + g_B(x^0, \delta^0)\delta^0 \tag{40}$$

The corresponding linear system is

$$\begin{aligned} \Delta\dot{x} &= A\Delta x + B\Delta\delta \\ \Delta y &= H_x \Delta x \end{aligned} \tag{41}$$

Under the construction of g_B, the trim condition is the same as the trim for the actual system. Moreover, this linear system is the same as the actual system with the exception of the linear control input map *B*.

For an equal number of controls and control variables, i.e. $l = m$, the inner loop of the dynamic inversion control produces m closed-loop poles at $s = 0$ and $n - m$ closed-loop poles at the transmission zeros of the open-loop system [9]. These $n - m$ closed-loop poles are furthermore unobservable to the outer-loop control. To promote internal stability, it is important that there are no right half plane transmission zeros. When $l > m$, the transmission zeros of an equivalent system can be used to determine internal stability.

The closed inner-loop can be described as

$$\begin{aligned} \Delta\dot{x} &= A\Delta x + BWB^T H_x^T (H_x BWB^T H_x^T)^{-1}\Delta z \\ \Delta z &= \Delta\dot{y}_{des} - H_x A\Delta x \\ \Delta y &= H_x \Delta x \end{aligned} \tag{42}$$

It can be shown that this same closed-loop system can be realized with dynamic inversion using the following $m \times m$ square system

$$\begin{aligned} \Delta\dot{x} &= A\Delta x + BWB^T H_x^T \delta_{psuedo} \qquad \delta_{psuedo} \in R^m \\ \Delta y &= H_x \Delta x \end{aligned} \tag{43}$$

where $\delta_{psuedo} = (H_x BWB^T H_x^T)^{-1}\Delta z$. As a result, the closed-loop system of (42) will have m poles at $s = 0$ and $n - m$ poles at the transmission zeros of the system in (43). It is clear from (43) that both the choice of control variables (i.e. H_x) and the weighting W influence the transmission zeros of (43) and therefore the closed-loop poles of (42). Either may have to be changed to preserve closed-loop stability.

Examples

Eleven control effectors are used in the following examples, but four of the controls are unilateral leaving 9 effective controls. These effective controls are left elevon, right elevon, symmetric pitch flap, all-moving tip (AMT), spoiler-slot-deflector (SSD), left outboard leading edge flap, right outboard leading edge flap, pitch vectoring, and yaw vectoring. The two one-direction controls are the AMT and the SSD, both of which have left-side and right-side controls.

Yaw-Roll-Pitch Maneuver

The three control variables are defined in the vector

$$y = [q_b,\ p_s,\ \beta - 0.2r_s] \tag{44}$$

where the longitudinal variable is pitch rate, the lateral variable is stability axis roll rate, and the directional variable is a linear combination of sideslip and stability axis yaw rate. The latter case illustrates that any linear combination of states can be used. With this combination of control variables and definitions in eq. (19), the matrix *H* (eq. 4) becomes

$$H = \begin{bmatrix} 0 & 1 & 0 & 0 & 0 \\ 0 & 0 & 0 & 1 & 0 \\ 0 & 0 & 1 & 0 & -0.2 \end{bmatrix} \tag{45}$$

which is used with equation (20) to define the h_x matrix (eq. (18)). Values for parameters that define the desired dynamics (eq. (5) - (7)) are listed in table 1.

In the lateral channel, a second outer loop was wrapped around the first outer loop for p_s to control bank angle ϕ. A simple first order response expressed by

$$\dot{\phi}_c \approx \omega_{phi}\left(\delta_{\phi,c} - \phi\right) \tag{46}$$

$$\delta_{lat} = \left(\dot{\phi}_c - \left(q_b \sin\phi + r_b \cos\phi\right)\tan\theta\right)\cos\alpha \tag{47}$$

where bandwidth ω_{phi} was used with a value shown in table 1. δ_{lat} represents the stability-axis roll rate command and is given in eq. (6) for the first outer loop.

Table1. Command Model Parameters

Parameter	Value	Parameter	Value
ς_{lon}	0.7	ω_{lat}	2
ω_{lon}	5	ς_{dir}	0.7
$\omega_{n,lon}$	3	ω_{dir}	3
K_{lon}	1/3	ω_{phi}	0.75

In the example problem, the airplane was trimmed straight and level at 25000 feet and Mach 0.7. A directional channel doublet of amplitude 5 degrees was commanded during the first 5 seconds. At 7.5 seconds into the simulation, a 50 degrees bank angle step was commanded, and between 11 and 16 seconds a

5 deg/sec pitch doublet was commanded. In addition, at 0.05 second into the simulation, the throttle was increased by 60 degrees above the trim value. This large increase in throttle along with the downward direction of the velocity vector caused Mach number to increase from 0.7 to 0.9 over the 20-second simulation.

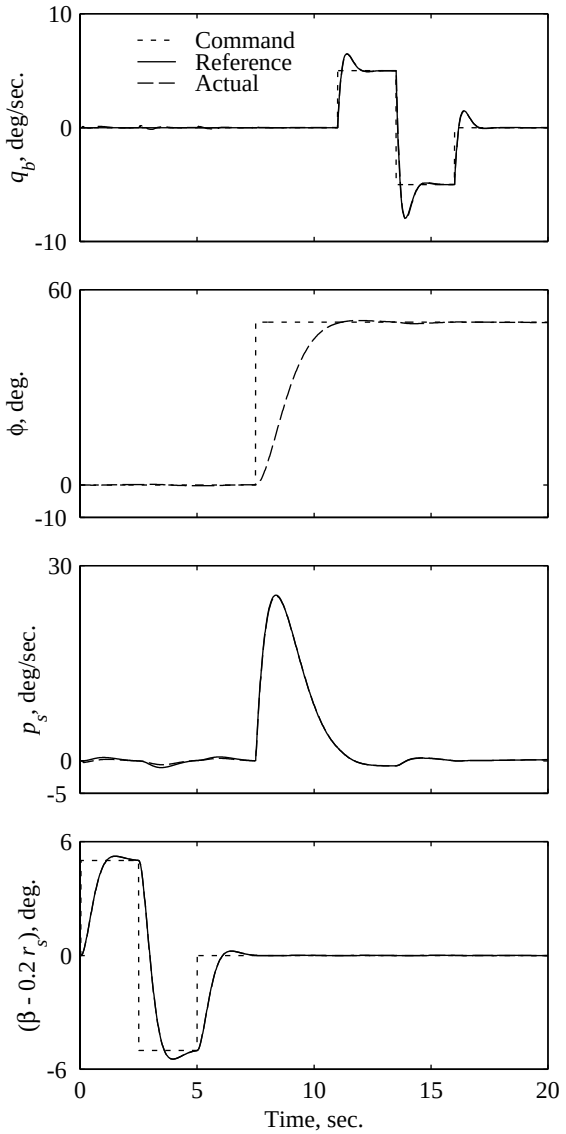

Figure 6. Yaw-roll-pitch maneuver.

Three variables are shown in the four plots in figure 6. The short-dashed lines represent input commands y_c, the solid lines represent reference signals from the open-loop command models, and the long-dashed lines represent the control variables. The top plot is for the longitudinal doublet command. The q_b response almost perfectly duplicates the reference response. The second plot is for the ϕ response and the generated error is the command for the p_s response that is shown in the third plot. Finally, the directional doublet command and response is shown in the fourth plot. In both the third and fourth plots, the response is a very close replica of the reference response. Note that there isn't any reference response for the bank angle response.

High Angle-of-Attack (Alpha) Response

The next example illustrates how a command-model variable can be changed to investigate the achievable dynamics, using a high angle-of-attack (α) maneuver which is illustrated in figure 7. The trim condition is straight and level at 25000 feet and Mach 0.4. The longitudinal control variable is changed to the linear combination $\alpha + 0.2 q_b$ [5]. In this example y_c is ramped in one second from a trim at $\alpha \approx 12^\circ$ to maximum where trim $\alpha \approx 42^\circ$. That value is held until 5 seconds into the simulation and then is ramped back to the initial trim 7 seconds into the simulation where y_c remains constant until the end. The throttle was also increased at 0.04 second by 60 degrees above the trim value.

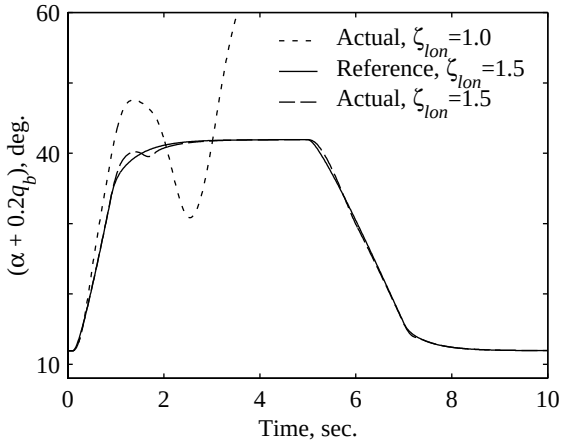

Figure 7. High angle-of-attack maneuver.

For the first command model where $\varsigma_{lon} = 1.0$, the short-dashed line represents an unstable response with all other command dynamics remaining the same as shown in table 1. All the longitudinal controls become position and rate saturated, and clearly the desired dynamics cannot be achieved. For the second command model with $\varsigma_{lon} = 1.5$, the solid and long-dashed lines represent the reference signal and closed-loop response, respectively. Perfect tracking is achieved for most of the simulation, except when y_c suddenly changes slope. At those times, the left and right elevons and the pitch thrust vectoring effectors temporarily position saturate, but the symmetric pitch flap remains within the allowable region. Rate saturation also occurs

temporarily in all the longitudinal controls. During this simulation run, Mach decreased to approximately 0.18. Between the two examples, a wide range of dynamic pressure and angle-of-attack variation has been demonstrated.

Although not shown, various failure cases were simulated for all of the different configurations to evaluate the approach described earlier in this paper. Excellent performance was achieved when the desired dynamics remained within the achievable range.

Concluding Remarks

A generic nonlinear aircraft simulation is used to evaluate an aircraft's achievable dynamics and control power requirements during maneuvers. Nonlinear dynamic inversion provides the theoretical underpinnings of the approach forcing designated control variables to track command-model signals. Under the assumption of internal stability, perfect tracking is theoretically possible when i) all necessary variables including forces and moments can be continually extracted from the simulation, ii) all controls are linearly related to their generated forces and moments, and iii) controls do not exceed their position and rate limits. In this paper, (i) was satisfied and (ii) was not satisfied whereas excessive violations of (iii) characterized dynamics outside the achievable set. In spite of the difficulties with (ii), near perfect tracking was obtained with the introduction of a linear control map approximation. This approximation roughly satisfied (ii) over each integration time step. Its construction, using only existing simulation data, greatly enhanced the overall efficiency of the approach.

Other complications dealt with include features and applications common to current aircraft and simulation usage. These include effectors that operate only with positive (or negative) deflections, table look-up vs. functional formulations of control forces and moments, effector failure accommodation, and the blending of multiple effectors when the number is greater than the number of control variables. Furthermore, internal stability, a fundamental assumption of dynamic inversion theory, is shown here to be a function of control variable definition and control allocation.

Two examples are used to demonstrate excellent tracking in all three axes over a wide range of dynamic pressure and angle-of-attack when sufficient power is available. The high angle-of-attack example illustrates how the choice of command model influences the control power required and determines the achievable dynamics.

Acknowledgement

The nonlinear simulation ATLAS used in this research is the property of the Flight Controls Branch of Lockheed Martin Tactical Aircraft Systems.

References

[1]Aviation Safety and Pilot Control: Understanding and Preventing Unfavorable Pilot-Vehicle Interactions. National Academy Press, Washington, D.C., 1997.

[2]Klyde,D.H.; McRuer D.T.; and Myers,T.T.: Unified Pilot-Induced Oscillation Theory Vol.I: PIO Analysis with Linear and Nonlinear Effective Vehicle Characteristics, Including Rate Limiting. WL-TR-96-3028, 1995.

[3]Smith, P. R.: Functional Control Law Design Using Exact Non-Linear Dynamic Inversion. *AIAA Atmospheric Flight Mechanics Conference*, 94-3516-CP, pp. 481-486, August 1994.

[4]Smith, P. R., and Patel, Y: Translational Motion Control Of VSTOL Aircraft Using Nonlinear Dynamic Inversion. *AIAA Atmospheric Flight Mechanics Conference*, 95-3452-CP, pp. 238-252, August 1995.

[5]Ostroff, A. J.: *Study of a Simulation Tool To Determine Achievable Control Dynamics and Control Power Requirements With Perfect Tracking.* NASA/TM-1998 -208699, August 1998.

[6]Military Standard Flying Qualities of Piloted Aircraft. MIL-STD-1797A, Jan. 30, 1990.

[7]Dorsett, K.M.; and Mehl, D.R.: Innovative Control Effectors (ICE). WL-TR-96-3043, January 1996.

[8] Scott, Michael A.; Montgomery, Raymond C.; and Weston, Robert P.: Subsonic Maneuvering Effectiveness of High Performance Aircraft Which Employ Quasi-Static Shape Change Devices. *SPIE 5th Annual International Symposium on Smart Structures and Materials*, San Diego, USA, March 1-6, 1998.

[9]Honeywell Technology Center; Lockheed Martin Skunk Works and Lockheed Martin Tactical Aircraft Systems: Application of Multivariable Control Theory to Aircraft Control Laws. WL-TR-96-3099, Final Report for March 1993 to March 1996, May 1996.

[10]Bugajski, D.J.; Enns, D.F.; and Elgersma, M.R.: *A Dynamic Inversion based Control Law with Application to High Angles of Attack Research Vehicle*, AIAA Guidance, Navigation, and Control Conference, 90-3407-CP, pp. 826-836, August 1990.

[11]Roskam, Jan: Airplane Flight Dynamics and Automatic Flight Controls, Part I. Published by *Roskam Aviation and Engineering Corporation*, Ottawa, KS, 1979.